JOURNAL OF CATALYSIS 50, 530–540 (1977)

Preparation of Small Au–Pd Particles on Silica

Y. L. LAM AND M. BOUDART[1]

Stauffer Laboratories of Chemistry and Chemical Engineering, Stanford University, Stanford, California 94305

Received April 29, 1977; revised Agust 12, 1977

Small Au–Pd particles 2.0 to 4.5 nm in diameter were prepared by ion exchange of $[Au(en)_2]^{3+}$ and $[Pd(NH_3)_4]^{2+}$ with surface protons of silica gel to form a precursor, which was subsequently reduced in dihydrogen. The Mössbauer effect of ^{197}Au yielded direct evidence of alloy formation and suggested that alloy particles were of a uniform composition close to the composition of the whole alloy sample. Further, selective chemisorption and X-ray line broadening showed that the surface composition of the alloy particles was similar to the overall composition.

INTRODUCTION

Although catalysis by alloys has been commonplace since the Ostwald process, preparation and characterization of small alloy particles in the size range between 1 and 5 nm are recent developments (*1*).

For very small particles, one of the few methods available to assess alloy formulation when X-ray diffraction becomes inadequate is Mössbauer effect spectroscopy (MES). Recent reviews discuss the use of MES in the characterization of Pt–Fe and Pd–Fe alloys (*2*, *3*).

Another alloy of considerable interest is Pd–Au. First of all, Au has an isotope for MES. Second, Au is well known for its inertness among Group Ib metals (*4*), so that, on a Au–Pd surface, the Au atoms may be considerably less active than the Pd atoms for adsorption and catalysis, and Au may be viewed in first approximation as an inert diluent. Third, Au–Pd alloys are perhaps the best example of monophasic random alloys forming a continuous series of solid solutions. The standard free energy of alloy formation is negative from 298 to 573 K (*5*). Therefore, upon equilibration of Au–Pd alloy at about 573 K, a single phase is expected to be formed. Both Pd and Au have the same fcc structure with lattice parameters of 0.3890 and 0.4078 nm, respectively. The Au–Pd alloys have lattice parameters with only very small deviation from the Vegard Law (*6*). Since metallic radii are similar and heats of vaporization of the two metals are nearly the same, the surface composition under vacuum is expected to be close to that of the bulk (*7*).

EXPERIMENTAL

The gases used were purified by procedures summarized in Table 1. The detailed study of the genesis of the alloys is presented elsewhere (*8*). Concisely, the sample preparation consisted of three consecutive steps. First, the salt $[Au(en)_2]Cl_3$ was prepared by the method of Block and Bailar (*8*). Second, a weighed amount of silica (Silica Gel Grade 950 from Davison, specific surface area: 700 $m^2\ g^{-1}$, specific pore volume: 0.4 $cm^3\ g^{-1}$) was warmed to 343 K in aqueous ammonia of about pH 11. The amount of solution was adjusted to 20 cm^3/g of silica. The appropriate amount

[1] To whom correspondence should be addressed.

ISSN 0021 9517

of $[Au(en)_2]Cl_3$ was dissolved in a calculated amount of 0.01 *M* solution of $[Pd(NH_3)_4]Cl_2$ to give the desired alloy composition. The concentration of $[Au(en)_2]Cl_3$ was never allowed to exceed 0.01 *M*. The well-mixed solution of complex salts was added dropwise into the slurry of silica at a rate of approximately 6 cm^3/min. At this rate, the temperature of the slurry never fell below 335 K. After addition of the solution, the slurry was maintained at 343–335 K for 1 h and then was cooled to room temperature. The treated silica, hence designated as the precursor, was filtered and thoroughly washed with at least three portions (5–6 cm^3/g of silica) of double-distilled water.

Finally, the precursor was loaded into a Pyrex glass cell and was evacuated by a diffusion pump at 333 K overnight. After the cell was cooled down to room temperature, dihydrogen was passed over the precursor at a space velocity of about 5 s^{-1}. The precursor was slowly heated to 423 K and then was maintained at that temperature for 3 more h before being cooled down to room temperature in flowing dihydrogen. After evacuation at room temperature for 0.5 h, the sample was slowly exposed to air and then was stored. A portion of the sample was submitted to elemental analysis by atomic absorption.

For comparison, a sample containing large Au particles about 20.0 to 100 nm in diameter and another sample containing Pd particles about 8 nm in diameter were also studied. The precursors of the Au and Pd samples were prepared by impregnation of $HAuCl_4$ and $Pd(NO_3)_2$ aqueous solutions, respectively, on the same silica support. Each precursor was dried and decomposed by the same schedule as used for the ion-exchange samples.

To examine the samples by MES, ^{197}Au sources were prepared by neutron activation of 97% ^{196}Pt foils (Oak Ridge National Laboratory). A ^{196}Pt foil (5 × 5 mm, 75 mg) was irradiated by a neutron flux of about 10^{19} cm^{-2} s^{-1} for 3.6 h in the test reactor of General Electric Co. at Vallecitos, Calif. After irradiation, the source was cooled for 18 h before being delivered to Stanford. The initial total activity at Stanford was estimated to be 70 mCi, of which 50% was due to the 77.7-keV MES transition.

TABLE 1

Purification of Gases

Gas	Source	Purity (%)	Further purification
H_2	Liquid Carbonic	99.93	Pd-diffused
O_2	Liquid Carbonic	99.5	Passed over a Linde 5A molecular trap at 195 K
He	Liquid Carbonic (Grade A)	99.995	Passed over hot Cu wire and then a liquid nitrogen trap
CO	Matheson	99.99	Passed over a Linde 5A molecular trap at 195 K

Two low-temperature dewars were employed in this study. A sample dewar was designed for *in situ* study of catalysts and had the unique property that the sample could be treated at high temperatures (600 K) and then cooled down to low temperatures (10 K) for MES while its gaseous environment was kept intact. The construction of this dewar has been fully described by Bartholomew (*9*). A source dewar was constructed for this study to interphase with the first. This dewar allows quick cool down of the source to 6–8 K. The design and operation of this dewar are described elsewhere (*3*). The complete setup of the two dewars during an experiment is shown in Fig. 1. The essential specifications of the Mössbauer spectrometer and the method of data analysis are summarized in Table 2. Details are given elsewhere (*9*). All spectra were fitted by means of Lorentzian peaks.

About 3 g of a sample was loaded into the sample chamber of the sample dewar and then was evacuated at 353 K for 1 h. It was exposed to 101 kPa of dihydrogen at room temperature for 0.5 h and then was evacuated at room temperature for

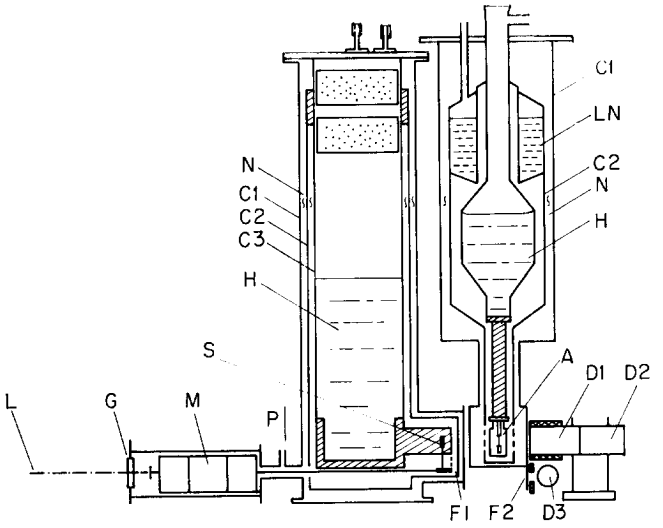

FIG. 1. Experimental set up for a Mössbauer effect experiment. (A) Absorber, (C1) outer cylinder, (C2) copper heat shield, (C3) inner stainless steel cylinder, (D1) NaI(T1) scintillation detector, (D2) preamplifier for D1, (D3) $Kr(CO_2)$ proportional counter with preamplifier, (F1) ^{57}CO source (ASA), (F2) Fe foil for calibration, (G) Plexiglas window, (H) liquid He, (LN) Liquid N_2, (L) He–Ne laser source (ASA), (M) K-3 linear motor (ASA), (N) Super-insulation (NRC-21), (P) to pump, (S) $^{197}Au/Pt$ source (GETR).

0.5 h. It was cooled down to 20 K for Mössbauer effect study. In addition, the sample with the highest Pd-to-Au ratio studied was rereduced at 573 K for 1 h in the sample chamber. Then, without evacuation, He gas was introduced into the sample chamber with a space velocity of 1 s^{-1}. After purging for 2 h with He, the sample was cooled down under 101 kPa of He to 20 K. The purpose of this He treatment was to free the surface of the sample from adsorbed gas which might affect the isomer shift of Au.

TABLE 2

Mössbauer Spectroscopy: Instrumental Details and Method of Data Reduction

Velocity calibration	Laser Interferometry (ASA), cross calibrated by a $^{57}CO/Cu$ source and an iron foil absorber (ASA)
Drive mode	Constant acceleration, "normal mode"
Curve-fitting method	Variable metric minimization program from Argonne National Laboratory
Isomer shift convention	Reported with respect to the Au/Pt source, positive sign for source approaching absorber
Error estimation	From the standard deviation of the derived parameters calculated by the curve-fitting program.

Next, X-ray diffraction patterns were obtained by a Picker X-ray diffractometer. Nickel-filtered Cu radiation was collimated by 1–2° Soller slits. For samples that gave resolved diffraction patterns, X-ray line broadening was studied. To calculate the linewidth (or width at half-maximum intensity), instrumental broadening was corrected for with crystalline α-quartz at $2\theta = 26.66°$ and the Warren method of instrumental broadening correction. The X-ray particle size was calculated from the Scherrer equation with a shape factor of 0.9 (*10*).

The apparatus for adsorption measure-

TABLE 3

Composition of Samples on Silica Support

Designation	Amount of Au in Pd–Au alloy (mol%)	Total metal content (μmol g^{-1})
L(0)	0	131
L(20)	19.4	125
L(40)	40.2	114
L(60)	54.2	122
L(80)	66.7	133
L(100)	100	122
H(0)	0	227
H(20)	20.8	249
H(40)	42.1	272
H(60)	59.0	225
H(80)	79.7	236
H(90)	88.0	196
H(100)	100	216
E(20)	23.0	736
E(52)	53.0	460
E(100)	100	380

ments was a conventional high-vacuum manifold connected to a high-precision Texas Instruments pressure gauge (*11*). Prior to characterization by H_2 or CO or O_2 chemisorption, each alloy sample was re-reduced at 573 K for 3 h and then was evacuated to about 10^{-7} kPa for 1 h at 573 K to prepare the samples for chemisorption. It was then cooled to room temperature for about 0.5 h, and an adsorption isotherm was obtained. Then, the sample was evacuated at room temperature for 0.5 h, and a backsorption isotherm was obtained. For a pure Pd sample, the procedure was the same as that for the alloy samples except that the reduction and evacuation at 573 K were carried out at 673 K.

Dihydrogen titration of preadsorbed oxygen was performed following dioxygen adsorption isotherms. Simply, the oxygen not strongly held by the sample was removed by evacuation at room temperature for 1 h. Dihydrogen was then allowed to contact the sample. Dihydrogen backsorption was also carried out as after dihydrogen adsorption.

RESULTS

Samples

The samples used in this study and subsequent papers are listed in Table 3 with convenient code numbers denoting the percentage of gold that was aimed at in the preparation. Letters L and H stand for metal loading in the vicinity of 125 and 250 μmol g^{-1} of sample. The letter E (excess) stands for a metal loading exceeding 380 μmol g^{-1}. Except for sample L(80), the results of the elemental analysis shown in Table 3 are in good agreement with the nominal Au percentage. A possible explanation for the deviation between the nominal and the determined compositions for L(80) is as follows. Instead of using freshly prepared Au-amine salt, the amine salt used had been prepared 10 days before exchange. It was dissolved in water and was filtered to remove possible photodecomposed Au salt. Filtration loss or photodecomposition of the Au complex to Au metal might have occurred. Hence the Au complex solution was diluted. Such a deviation from nominal composition was circumvented in later preparations by using freshly prepared complexes for exchange (1 or 2 days old).

Physical Data

Tables 4 and 5 summarize the MES parameters for the samples. Literature values for bulk Au and Au–Pd alloys and parameters for an Au foil standard are also listed for comparison (*12–14*). The isomer shift of the spectra of the Au foil was in good agreement with the literature value. From the published value of the natural linewidth of Au and the effective thickness of the Au foil, an experimental linewidth, Γ_e, of 2.34 ± 0.05 mm s^{-1} was

TABLE 4

MES Parameters of Supported Au Samples and Au Foils

Sample	δ^a (mm s^{-1})	Γ^b (mm s^{-1})	Dip (%)	Ref.
Au foil	−1.33	2.43	8.36	This work[c]
Au foil	−1.29	2.31	6.67	This work[c]
10 wt% Au/SiO_2 (20–100 nm)	−1.34	2.36	5.47	This work[c]
ME(100) (3.0 nm)	−1.22	3.42	4.88	This work[c]
Au	−1.25	2.30	—	(14)
10 wt% Au/MgO (500 nm)	−1.30	2.33	3.37	(13)
10 wt% Au/η-Al_2O_3 (10–200 nm)	−1.30	2.31	6.80	(13)

[a] Isomer shift.
[b] Linewidth.
[c] Error estimate in δ and Γ_e: ± 0.05 mm s^{-1}.

expected (*12*). The experimental value was in agreement with that expected. The spectrum obtained from large Au particles yielded an isomer shift and a linewidth similar to the corresponding parameters of the Au foil standard. By contrast, the spectrum from small Au particles, E(100), yielded a linewidth of 3.42 ± 0.05 mm s^{-1}, 49% broader than the Γ_e of the Au foil standard. This broad-line spectrum was expected since the Au atoms on the surface region of a small Au particle can assume sites of different local environments. This leads to a range of isomer shifts. Further, deviation from cubic symmetry at the surface gives a quadrupole splitting of the nuclear states. Unresolved quadrupole splitting also contributes to line broadening.

The isomer shifts of E(20) under He and of E(52) covered with hydrogen compared favorably with the values from bulk samples. The comparison is illustrated in Fig.

TABLE 5

MES Parameters of Supported Au–Pd Samples and Bulk Au–Pd Alloys

Sample	δ^a (mm s^{-1})	Γ^b (mm s^{-1})	Dip (%)	$\Gamma_x - \Gamma$ (mm s^{-1})	$(\Gamma_x - \Gamma)/\Gamma$
E(100)	−1.22	3.41	4.88	—	—
E(52) hydrogen covered	−0.32	3.92	3.66	0.41	0.15
E(20) under He	+0.41	3.44	1.20	0.04	0.01
Bulk samples[c]					
Au	−1.25	2.30	—	—	—
50 atom% Au	−0.22	2.50	—	0.20	0.10
20 atom% Au	+0.45	2.50	—	0.20	0.10

[a] Isomer shift.
[b] Linewidth (x: for alloy).
[c] Reference (*14*), Γ_e estimated from the reported graph. Uncertainty in δ and Γ_e in the supported samples: ± 0.05 mm s^{-1}.

2. The Mössbauer spectra are shown in Fig. 3.

The isomer shift of E(20) in He was slightly more positive than that of the same sample covered by hydrogen. Since the amount of hydrogen adsorbed on E(52) was relatively small, the effect of the adsorbed hydrogen on that sample may be neglected.

The linewidth of the lines for alloy particles was compared with the linewidth for small Au particles. The linewidth for bulk alloy was also compared with that for bulk Au. Values of line broadening, defined as Γ_e (alloy) $-$ Γ_e (Au), and the relative line broadening, defined as [Γ_e (alloy) $-\Gamma_e$ (Au)/Γ_e (Au)], are summarized in Table 5.

For both the L and the H series of samples, the X-ray diffraction patterns were generally extremely diffuse, indicating that the metals were in a highly dispersed state. For the E series of samples, diffraction patterns were observed. Figures 4a and 4b show the diffraction patterns for E(20) and E(52), respectively. The peak positions shifted from pure Au or pure Pd as expected for their compositions. With a graphite internal standard, these shifts due to alloy formation were estimated. They are shown in the figures. Finally, for Au only samples with Au loading from 122 to 380 μmol g^{-1} (from 2.4 to 7.5 wt%), an X-ray particle size of about 3.0 nm was obtained. This is the first time that supported Au particles of this small range have been reported.

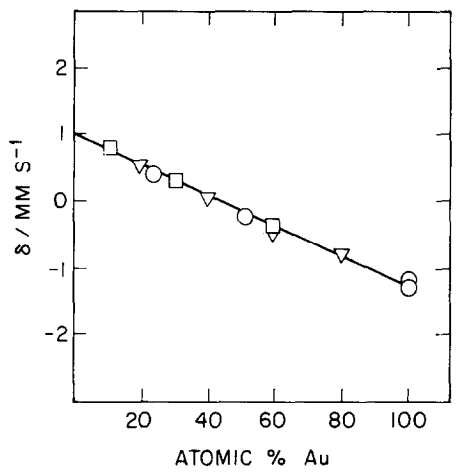

FIG. 2. Evidence for alloy formation: Isomer shift (δ) of bulk Au–Pd alloys and supported Au–Pd alloys. (∇) Typical values from Longworth (*14*); ($\square$) typical values from Roberts *et al.* (*12*); ($\bigcirc$) this work.

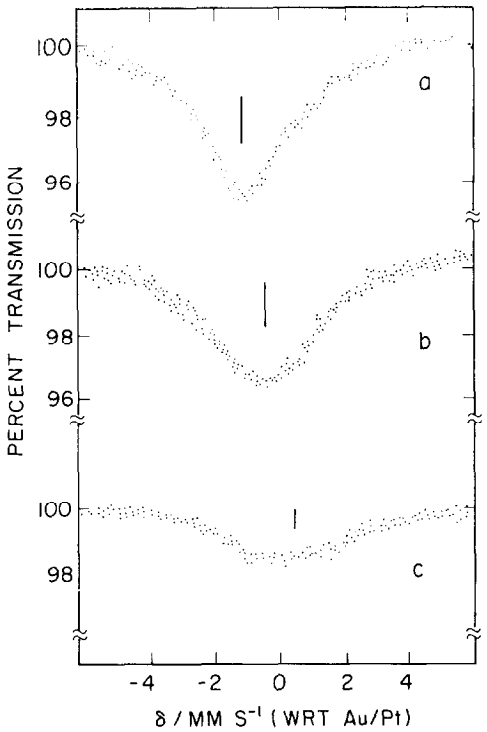

FIG. 3. Mössbauer effect spectra. (a) ME(100); (b) ME(52) covered by hydrogen; (c) ME(20) in He gas.

Adsorption of Gases

Figures 5 and 6 show sets of typical gas uptake isotherms. The amount of gas taken up was obtained by extrapolation to zero pressure. The amount of gas held strongly on the surface was obtained by the difference between the total uptake and the amount backsorbed. Figures 7a to d summarize the uptake of gas per Pd atom. Table 6 shows that, for a given sample,

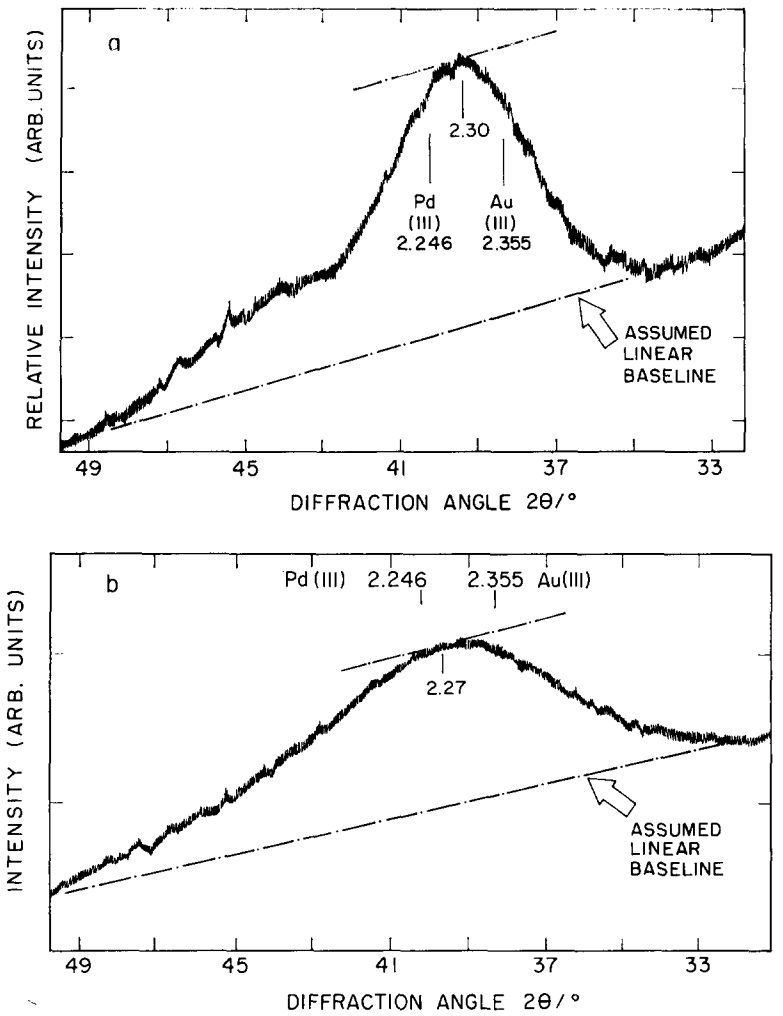

FIG. 4. X-Ray diffraction patterns. (a) ME(20); (b) ME(52).

the ratio of the amounts of O_2 to CO taken up was approximately constant as a function of alloy composition, while that of H_2 to CO decreased with increasing Au-to-Pd ratio.

DISCUSSION

As pointed out by Bartholomew and Boudart (*15*) three pieces of information are essential for defining a binary alloy A–B on a support: first, evidence for alloy formation; second, the overall dispersion of the metal, defined as the ratio of the total number of surface metal atoms to the number of all metal atoms present; and, third, the surface composition of the alloy which can be obtained from the dispersion of component A, defined as the ratio of the number of surface A atoms to the total number of A atoms.

Physical and Chemical Evidence for Au–Pd Alloy Formation on SiO_2

Physical evidence for alloy formation was obtained for samples with high metal

loading, such as the E series. The X-ray diffraction pattern of each of these samples does not show more than one distinct metallic phase and the lattice parameter of the metallic phase agrees with that of an alloy of the desired composition. More quantitatively, the isomer shifts of these samples compare favorably with those of bulk alloys. The above observations not only verify alloy particle formation of SiO_2 for the E series of samples, but show that the methods of preparation and decomposition of the precursors lead to Au–Pd alloy formation.

More can be learned about the prepared alloy particles from the widths of the MES lines. The absorption line of an alloy is broader than that of pure Au simply because it is a superposition of absorption lines due to Au nuclei with different numbers and arrangements of Au and Pd neighbors. This broadening can be observed with bulk alloys (*14–16*). In addition, for small alloy particles, if the compositions of individual particles are significantly different from the average composition of all particles, or, if within each particle, there are regions with greatly different compositions, a further line broadening is expected. In the present case, the linewidth of the alloy particles is similar to that for small Au particles (Table 5). This suggests that alloy particles are formed with a uniform composition close to the average sample composition.

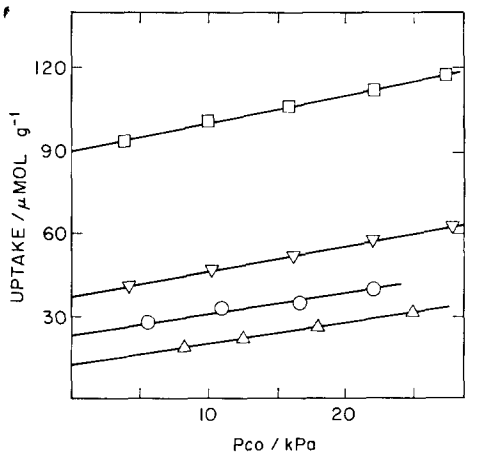

FIG. 5. Typical CO adsorption isotherms at room temperature; each sample had been evacuated at 573 K for 1 h. (□) L(20); (▽) L(40); (○) L(60); (△) L(80).

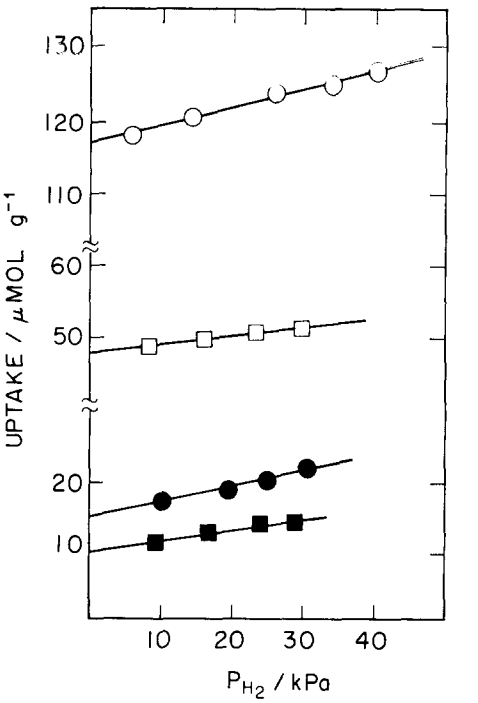

FIG. 6. Typical H_2 titration and backsorption and backsorption isotherms at room temperature. (○) L(20), titration total uptake; (●) L(20), backsorption; (□) L(40), titration total uptake; (■) L(40), backsorption.

Chemical evidence for alloy formation was obtained for samples with high or low metal loadings. Figures 7a and d show that the amounts of H_2, O_2, and CO that are strongly held on the Au–Pd samples fall rapidly as the Au-to-Pd ratio increases. Since Au does not adsorb gases strongly (*4, 17*), it is reasonable to divide the amount of gas taken up by the number of Pd atoms only. The fall of gas uptake per Pd atom is a consequence of several effects of alloy formation the relative importance of which will be discussed in the next section.

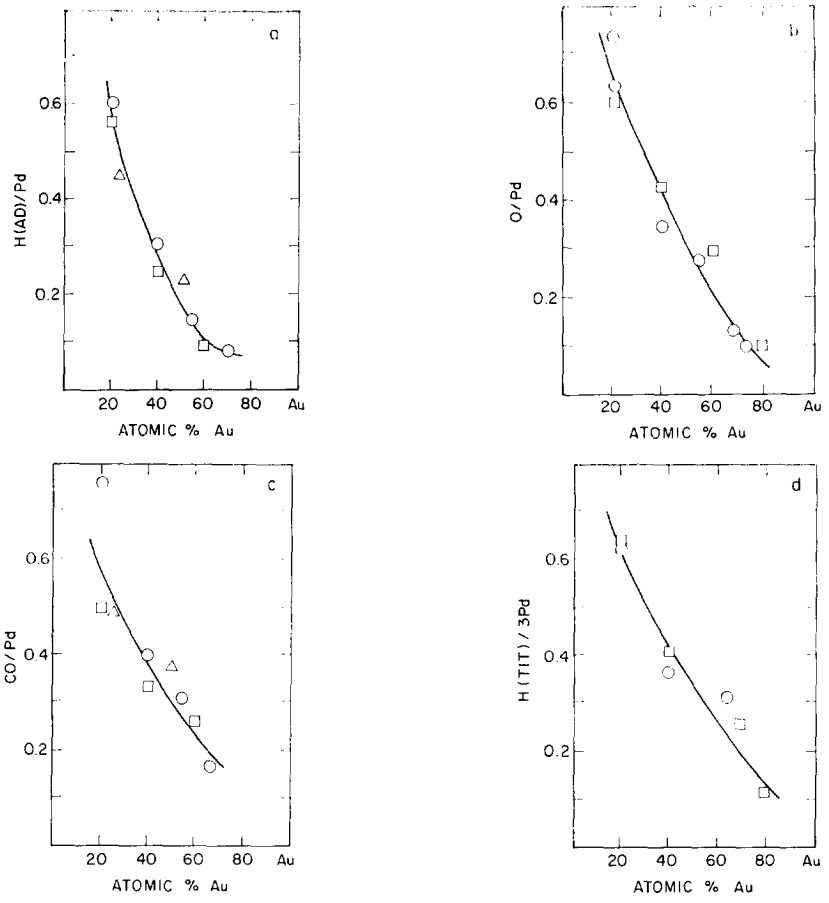

FIG. 7. Gas uptake as a function of total alloy composition. Diagrams: (a) H/Pd, (b) O/Pd, (c) CO/Pd, (d) H(titration)/3 × Pd. Samples: (○) L series, (□) H series, (△) ME series.

Palladium Dispersion, Overall Dispersion, and Surface Composition

The Pd dispersion of the alloys can be deduced from the amount of CO strongly held and the assumption that, on the average, one CO molecule is adsorbed on one surface Pd atom. This method yields values

TABLE 6

Ratios for Uptake of Gases at 295 ± 2 K

Sample	H_2/CO	O_2/CO
L(0)	—	0.52
L(20)	0.40	0.42
L(40)	0.39	0.44
L(60)	0.25	0.45
L(80)	0.26	0.50
H(0)	0.63	0.66
H(20)	0.57	0.61
H(40)	0.38	0.66
H(60)	0.17	0.57

TABLE 7

Comparison between Particle Size Estimations

Sample	Particle diameter (nm)	
	X-Ray	CO[a]
E(20)	1.5 ± 0.5	1.9 ± 0.2
E(52)	2.9 ± 0.6	2.3 ± 0.2
L(80)	3.2 ± 0.6	3.0 ± 0.3
H(80)	4.1 ± 0.8	4.7 ± 0.3

[a] Obtained from the assumptions that (i) 1 CO is adsorbed on 1 Pd surface atom and (ii) surface percentage composition similar to the bulk percentage composition.

of dispersion for pure Pd particles in good agreement with those determined by other techniques (*18*). Also, CO molecules are absorbed selectively and strongly on surface Pd atoms (*19*), as suggested from the work of Gerberich *et al.* on Au–Pd powders (*20*). However, on bulk Pd or Au–Pd samples, a CO-to-Pd (surface) ratio of 0.6 is favored (*17*, *20*, *21*). On small particles, there are presumably more atoms with low coordination numbers that can accommodate a larger number of CO molecules per atom. Hence, a larger ratio is reasonable. This situation is demonstrated for CO adsorption on Ru (*22*). Note also that the Pd dispersion may also be estimated from the oxygen uptake since the O_2-to-CO uptake ratio is approximately 0.5 for the alloys studied (Table 6).

The Pd dispersion of the alloys is equal to the overall dispersion if and only if surface composition is equal to bulk composition. Experimentally, for samples which resolved X-ray diffraction patterns, the particle size can be estimated both by X-ray line broadening and from the Pd dispersion from CO adsorption, with the assumption that surface and bulk compositions are equal. Table 7 shows that the results of the two methods are in good agreement. Theoretically, since Au and Pd have very close values of heat of vaporization and atomic size, surface and bulk compositions of an equilibrated Au–Pd alloy *in vacuo* are expected to be close to each other (*7*), although this may not be the case in the presence of chemisorbed gases (*23*) or even *in vacuo*, at least for bulk samples (*24*, *25*). At any rate approximate equality between surface and bulk compositions is expected generally for small particles. Consider, for example, a Au–Pd alloy with 50 atom% Au and a Pd dispersion of 50%. Now, suppose that instead of a Au dispersion of 50%, the Au dispersion is 100%. Then, the surface will contain 66.7% Au which is not too different from the value of 50% Au that would prevail if surface and bulk compositions were identical. A more thorough treatment of this effect has been considered by Williams (*26*). It may be concluded that, for the small particles used in this work, surface and subsurface compositions of Pd–Au alloys are substantially the same. Hence, to a first approximation we can equate Pd dispersion with overall dispersion. Then we find that the particle size of the alloy aggregate increases from 2.0 to 4.5 nm with increasing amounts of Au in the alloys.

We can now understand the decrease in gas uptake per Pd atom with increasing Au content (Figs. 7a to d). The main reason is that the alloys richer in Au are in the form of larger particles so that the fraction of Pd surface atoms decreases with increasing Au content. Besides, for a gas like H_2, which is adsorbed on Au–Pd less strongly than are O_2 or CO, the average number of hydrogen atoms held strongly by surface Pd atoms may decrease as the number of Au neighbors of Pd increases. This possibility is consistent with the studies of the thermal accommodation coefficient of neon on Au–Pd filament in the presence of H_2 (*27*) and the recent calculation of binding energy of H_2 on alloys by Van Santen (*28*). At any rate, the observed trend of H_2 uptake with increasing Au content is fully compatible with all the other chemical and physical facts reported in this paper. They all indicate formation of small alloy particles on silica gel.

ACKNOWLEDGMENT

Support of this work by ARPA Grant No. N00014-75-C-1171 through the Center of Materials Research at Stanford University is gratefully acknowledged.

REFERENCES

1. Sinfelt, J. H., *Accounts Chem. Res.* **10**, 15 (1977).
2. Dumesic, J. A., and Topsøe, H., *in* "Advances in Catalysis and Related Subjects," Vol. 26, p. 121. Academic Press, New York, 1976.
3. Garten, R. L., "Mössbauer Effect Methodology," Vol. 10. Plenum Press, New York, 1976.

4. See for example: Anderson, J. R., "Structure of Metallic Catalysts," pp. 21–25, Academic Press, New York, 1975.
5. Darby, J. B., *Acta Met.* **14**, 265 (1966).
6. Maeland, A., and Flanagan, T. B., *Canad. J. Phys.* **42**, 2364 (1964).
7. Williams, F. L., and Nason, D., *Surface Sci.* **45**, 377 (1974).
8. Lau, Y. L., Ph.D. Dissertation. Stanford University, Stanford, Calif., 1976.
9. Bartholomew, C. H., Ph.D. Dissertation. Stanford University, Stanford, Calif., 1972.
10. Klug, H. P., and Alexander, L. G., "X-Ray Diffraction Procedures," Chap. 9. Wiley, New York, 1954.
11. Hanson, F. V., Ph.D. Dissertation, Chap. 1. Stanford University, Stanford, Calif., 1976.
12. Roberts, L. D., Becker, R. L., Obenshain, F. E., and Thomson, J. O., *Phys. Rev.* **137**, 895 (1965); also Roberts, L. D., *in* "Mössbauer Effect Data Index" (J. G. Stevens and V. E. Stevens, Eds.). IFI Plenum, New York, 1973.
13. Delgass, W. M., Boudart, M., and Parravano, G., *J. Phys. Chem.* **72**, 3563 (1968).
14. Longworth, G., *J. Phys. C*, Met. Phys. Suppl. No. 1 (1970).
15. Bartholomew, C. H., and Boudart, M., *J. Catal.* **29**, 278 (1973).
16. (a) Kimball, C. W., *in* "Mössbauer Effect Methodology" (Gruverman, I. J., Ed.), Vol. 3, p. 3. Plenum Press, New York, 1967; (b) Preston, R. S., Lam, D. J., Nevitt, M. V., and Van Ostenburg, P. O., *Phys. Rev.* **149**, 440 (1966).
17. Hayward, D. O., *in* "Chemisorption and Reactions on Metallic Films" (J. R. Anderson, Ed.). Academic Press, New York, 1971, and references therein.
18. Benson, J. E., Hwang, H. S., and Boudart, M., *J. Catal.* **30**, 146 (1973).
19. Kugler, E., Lam, Y. L., and Boudart, M., to be published.
20. Gerberich, H. R., Cant, N. W., and Hall, W. K., *J. Catal.* **16**, 204 (1970).
21. Ford, R. R., *Advan. Catal.* **21**, 51 (1970).
22. Dalla Betta, R., *J. Phys. Chem.* **79**, 2519 (1975).
23. Williams, F. L., and Boudart, M., *J. Catal.* **30**, 438 (1973).
24. Jablonsky, A., Overbury, S. H., and Somorjai, G. A., submitted.
25. Burton, J. J., and Machlin, E. S., *Phys. Rev. Lett.* **37**, 1433 (1976).
26. Williams, F. L., Ph.D. Dissertation. Stanford University, Stanford, Calif., 1972.
27. Faron, M. J., and Teichner, S. J., *Rev. Hautes Temp. Refract.* **1**, 201 (1964).
28. Van Santen, R. A., *Surface Sci.* **53**, 35 (1975).